Int. J. Electrochem. Sci., 12 **(2017)** 11171 – 11180, doi: 10.20964/2017.12.40

International Journal of
ELECTROCHEMICAL
SCIENCE
www.electrochemsci.org

Short Communication

Facile Hydrothermal Synthesis of Manganese Dioxide/Nitrogen-Doped Graphene Composites as Electrode Material for Supercapacitors

Bin Huang, Chenling Huang, Yong Qian[*]

Jiangxi Engineering Research Center of Process and Equipment for New Energy, East China University of Technology, Nanchang 330013, P.R. China
[*]E-mail: yqianecit@163.com

Received: 6 August 2017 / *Accepted:* 12 October 2017 / *Published:* 12 November 2017

We report a simple and efficient approach for the *in-situ* decoration of manganese dioxide (MnO_2) nanoparticles onto nitrogen-doped graphene (NG) using polyvinylpyrrolidone (PVP) as the dispersing agent and stabilizer. The morphology and microstructure of the as-prepared MnO_2/NG composites were characterized by transmission electron microscopy and X-ray photoelectron spectroscopy. The results show that a uniform dispersion of MnO_2 nanoparticles with a mean size of about 10–20 nm was successfully anchored on the NG surfaces. Furthermore, the electrochemical capacitive behaviors of the MnO_2/NG hybrid materials were investigated by cyclic voltammetry (CV) and galvanostatic charge–discharge (GCD). The MnO_2/NG composites delivered a high specific capacitance of 302 F/g at 1 A/g in 1 M Na_2SO_4 electrolyte; they also showed good cycling stability with 88.9% retention rate of specific capacitance after 1000 cycles of charge and discharge. This study provides a rational device for designing high-performance MnO_2-based supercapacitors.

Keywords: Supercapacitor, manganese dioxide, nitrogen-doped graphene, electrode material

1. INTRODUCTION

In recent years, providing clean and renewable energy resources are highly desired for environmental pollution and exhaustion of fossil fuels [1, 2], and significant progress has been made in advanced and environmentally friendly energy storage equipment [3, 4]. Supercapacitor is a key electrochemical energy storage and conversion devices which is of high power density, long cycle life, and excellent reversibility [5]. Tremendous effort in this field has been devoted to the development of different electrode materials such as carbonaceous materials [6], conducting polymers [7], and transition-metal oxides [8]. Among them, transition-metal oxides, e.g., RuO_2, NiO, Co_3O_4, MnO_2, and Mn_3O_4, are widely used as active materials for pseudocapacitor electrodes because of their high

capacitance and fast redox kinetics [9-12]. Especially, MnO_2 is of crucial importance for supercapacitors because of its electrochemical behavior, low cost, low toxicity, high theoretical capacitance, and environmental compatibility [13].

Some effective methods were used to make unusual MnO_2-based material structures with desirable properties include polymer-assisted method [14], microemulsion method [15], hydrothermal reaction, thermal decomposition [16], and template method [17]. However, MnO_2 does not usually provide a high specific capacitance because of its poor electrical conductivity and electrochemical dissolution during the cycling [18]. To overcome these obstacles, carbon materials with a high electrical conductivity have been widely used as the supports for MnO_2-based materials to improve their conductivity and prevent the aggregation of metal species into larger particles [19]. Graphene has also been widely used in hybrid materials such as metal oxides and polymers to enhance the electrochemical activities because of its unique properties such as superior electrical conductivity, excellent mechanical flexibility, and high thermochemical stability [20].

Chemical doping with foreign atoms is an effective way to improve the intrinsic structures and tailor electronic properties [21]. More importantly, graphene materials with nitrogen doping (NG) have become a research hotspot because their atomic size and strong valence bonds are similar to those of carbon atoms. The doping of N atoms effectively changes the electronic state and electron transfer process, and increases the number of active sites for catalytic reactions than the pristine form. Thus, the doping of heteroatoms in graphene improves the electrical conductivity and electrochemical performance [22].

In this paper, we report a rapid and facile wet chemical method for the synthesis of MnO_2/NG nanocomposites via polyvinylpyrrolidone (PVP)-assisted by ethylene glycol solvothermal process. For this nanocomposite, NG mainly serves as a highly conductive support for improving the electrochemical performance of MnO_2/NG. The capacitance characteristics of the MnO_2/NG composites were investigated in detail; the results show that the hybrid materials have good electrochemical performance as the electrode materials of supercapacitors.

2. EXPERIMENTAL

2.1. Chemicals

Graphene oxide (GO) was purchased from Nanjing XFNano Technology Co., Ltd. (China). The other chemicals were of analytical grade and obtained from Aladdin reagent Co., Ltd. (China) and used as received without further purification. Water (18 MΩ cm^{-1}) used in all the experiments was prepared by passing through an ultrapure purification system.

2.2. Preparation of MnO_2/NG composites

A one-step reaction procedure was used to prepare the MnO_2/NG hybrid materials. In a typical preparation, 100 mg of GO and 50 mg of PVP were mixed and thoroughly dispersed in 200 mL of

deionized water in a three-necked flask at 50 °C with stirring for 6 h. Next, 40 mg of $MnSO_4 \cdot H_2O$ and 40 mg urea were added into the flask, and the mixture was further stirred for 1 h. Then, 2 mL of 30% H_2O_2 was gradually added to the mixture. After the stirring, the mixture was transferred to a stainless steel autoclave and placed in an oven preheated to 160 °C for 3 h. After cooling to 50 °C, the suspension was filtered using a filter with a pore size of 0.45 μm, and the resulting product was washed with deionized water and ethanol. The resulting product was finally annealed at 300 °C in nitrogen for 3 h.

2.3. Characterization

Transmission electron microscopy (TEM) images were recorded using a JEOL JEM-2010 transmission electron microscope at an acceleration voltage of 200 kV. X-ray photoelectron spectroscopy (XPS) was carried out using a Thermo Fisher X-ray photoelectron spectrometer equipped with Al radiation as the probe, with a chamber pressure of 5×10^{-9} Torr. The source power was set at 72 W, and the pass energies for survey and high-resolution scans were 200 eV and 50 eV, respectively. The analysis spot size was 400 μm in diameter.

2.4. Electrochemical measurements

Electrochemical measurements were performed using a CHI 660E electrochemical workstation (CH Instrument, Shanghai) equipped with a three-electrode system at room temperature. An Ag/AgCl electrode was used as the reference electrode, and a Pt plate was used as the counter electrode. The working electrode was prepared by mixing electroactive materials with PTFE and carbon black, and the weight ratio of composite:PTFE:CB was 80:10:10. During the preparation of working electrode, 10 mg mixture was pressed on a Ni foam (1×2 cm^2) and dried at 80 °C in a vacuum oven for 3 h. The electrochemical performance of the working electrode was evaluated by carrying out cyclic voltammetry (CV) and galvanostatic charge–discharge (GCD) tests.

3. RESULT AND DISCUSSION

The morphology of the as-prepared NG and MnO_2/NG nanocomposite was characterized using TEM. As shown in Figure 1A, the as-prepared NG nanosheets are transparent, randomly compact, and stacked together, exhibiting a uniform laminar morphology similar to crumpled silk veil waves. Figure 1B shows that the sizes of the MnO_2 nanoparticles (NPs) are in the range 10–20 nm and distributed throughout NG with a high surface coverage. Moreover, it is clear that PVP is the reducing and stabilizing reagent for the preparation of the MnO_2/NG composites in this system. All these results indicate that well-dispersed MnO_2 NPs uniformly distributed on the surface of NG sheets provide a large available surface and deliver the electrocatalytic activity.

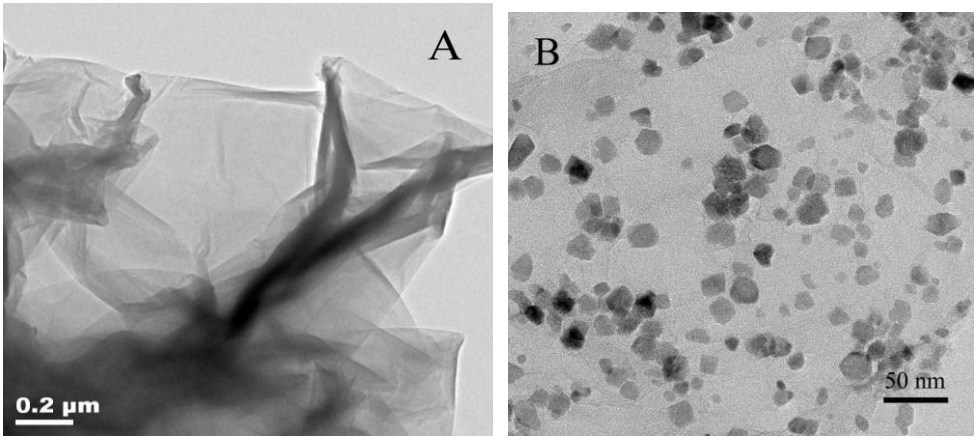

Figure 1. TEM images of (A) as-prepared NG and (B) MnO_2/NG composite

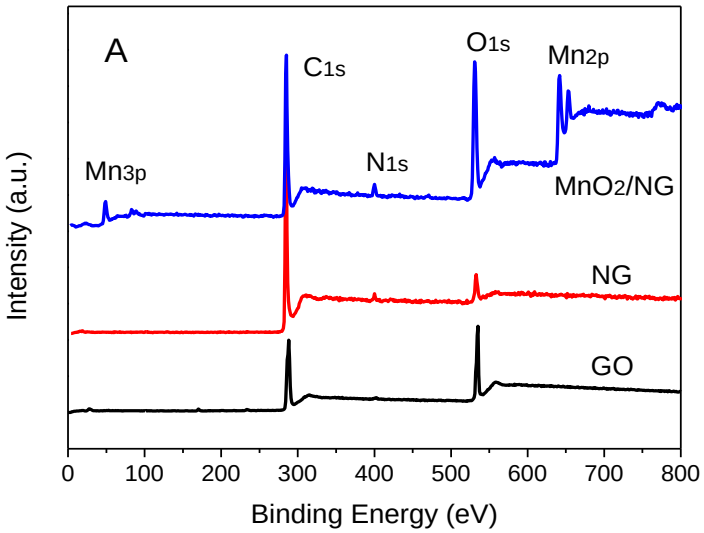

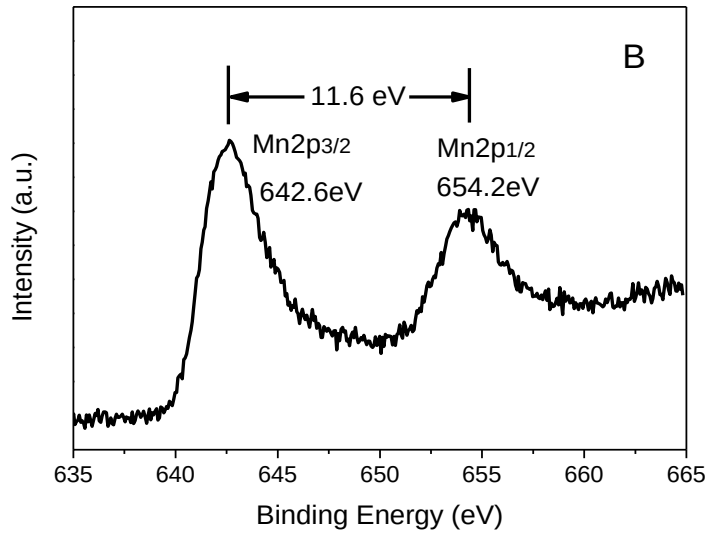

Figure 2. (A) XPS spectra of GO, NG and MnO_2/NG (B) high-resolution Mn2p XPS of the composite.

To obtain more information about the surface composition and chemical changes of GO, NG, and MnO_2/NG, XPS analysis was conducted. The wide-range XPS spectra are shown in Figure 2A. A new small peak for N1s was observed at ~400 eV in the XPS spectra of NG after the nitrogen doping and reduction of GO. In addition, the O1s peak of NG is much smaller than those of GO. This significant change indicates that the O-containing functional groups of the GO were partially removed or even disappeared in the NG. In the XPS spectrum of MnO_2/NG, the peaks for C1s, N1s, O1s, Mn2p (2p3/2, 2p1/2), and Mn3p were observed, indicating that the MnO_2 NPs anchored on the graphene surface. Figure 2B shows the high-resolution XPS spectra of Mn2p. Two characteristic peaks are located at binding energies of 654.2eV and 642.6eV, and a spin-energy separation of 11.6 eV was observed between the two peaks, similar to a previous report for Mn 2p3/2 and Mn 2p1/2 in MnO_2 [23]. These results confirm that the composite material is composed of NG and MnO_2.

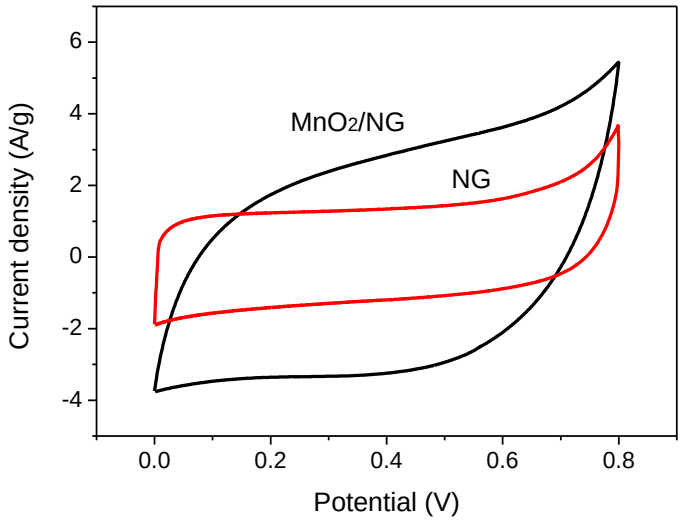

Figure 3. CV of NG and MnO_2/NG composite electrodes at a scan rate of 20 mV/s in 1 M Na_2SO_4

CV is a very effective method for characterizing the supercapacitive performance of electrode materials. The NG and MnO_2/NG composite electrodes were further evaluated by CV measurements, and the CV curves at 20 mV/s in 1 M Na_2SO_4 are shown in Figure 3. The CV profiles exhibit almost rectangular shapes without clear redox peaks in the applied potential window from 0 to 0.8 V, indicating excellent capacitive behavior of the electrode materials. As shown in Figure 3, the rectangular area of the CV loop of the MnO_2/NG composite electrode is significantly larger than that of NG electrode. In contrast to NG, we assume that the pseudocapacitance of MnO_2 phase and partially the intrinsic electrical double-layer capacitance of NG contribute to the enhancement of the electrochemical performance of the MnO_2/NG composite. Hence, the introduction of NG in the composites not only acts as the supports for MnO_2 NPs, but also as the electronic conductive bridges. MnO_2 can work well with graphene to provide a fast transportation of electrons throughout the entire electrode matrix.

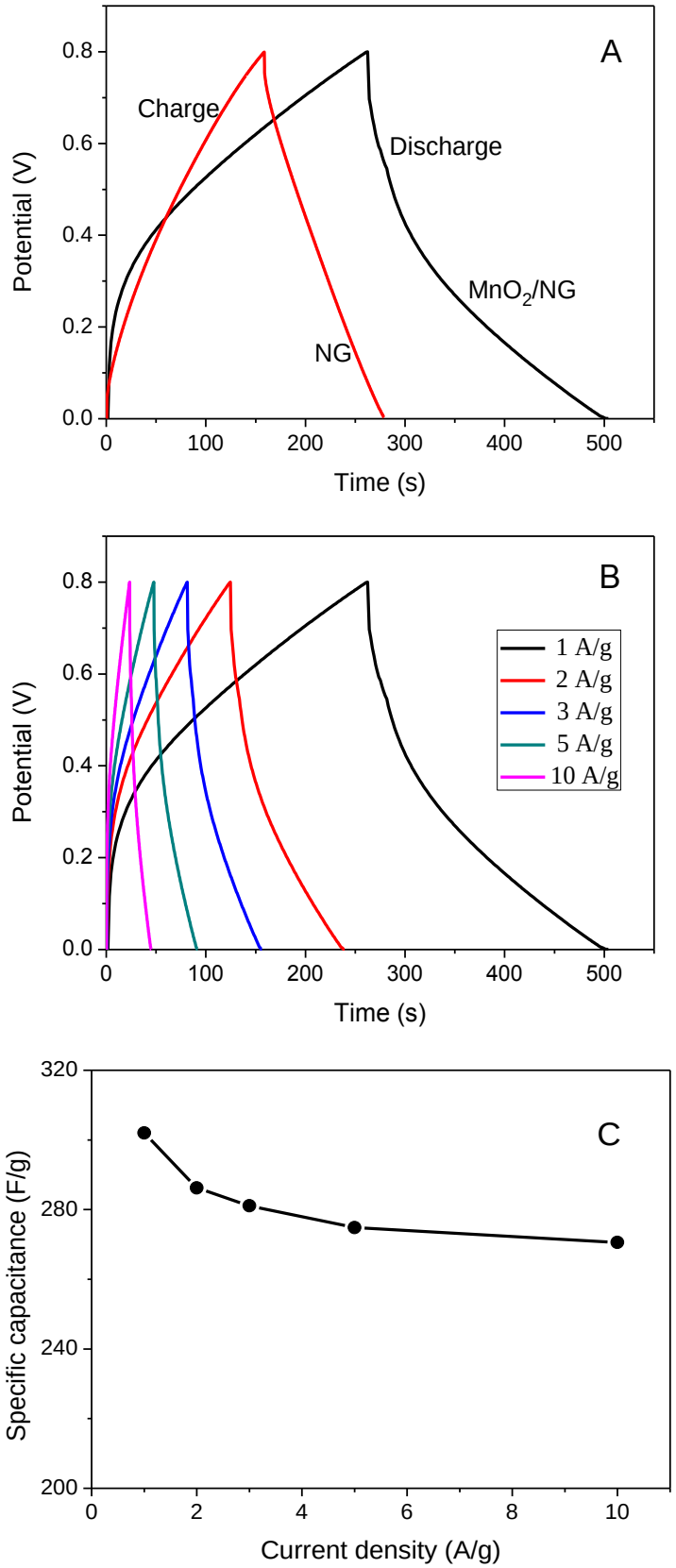

Figure 4. (A) GCD curves of NG and MnO_2 /NG at 1A/g, (B) GCD curves of MnO_2/NG in different current density, (C) relationship between the specific capacitance of MnO_2/NG in different current density

Further, GCD measurements were carried out to evaluate the potential applications of NG and MnO_2/NG as the electrode materials for supercapacitors. Figure 4A shows the GCD curves of NG and MnO_2/NG electrodes at a current density of 1 A/g. First, the GCD curve of NG exhibited an almost straight and symmetric charge–discharge curve. This result indicates that NG has good electrochemical reversibility during the charging and discharging steps. For comparison, the GCD curve of MnO_2/NG composites has a slight curvature as shown in Figure 4A, indicating that MnO_2/NG electrode material has a typical Faraday pseudocapacitance curve. The specific capacitances (Cs) were determined as follows: Cs = (It)/(mV), where I is the constant discharge current, V is the potential window, t is the discharge time, and m is the mass of the active material in the electrode. The MnO_2/NG delivered a specific capacitance (Cs) of 302 F/g at 1 A/g, much higher than that of NG (150.25 F/g). This result is consistent with the calculation from CV loops (Figure 3) and also shows that MnO_2 plays a critical role in improving the Cs. Figure 4B shows the GCD of MnO_2/NG electrode at different current densities ranging from 1 to 10 A/g. The time of charging−discharging procedure gradually increased with the decrease in current density. Such a trend can be attributed to the sufficient insertion or release of Na^+ ions during the charging and discharging steps. Figure 4C shows the relationship between Cs and current density of the MnO_2/NG electrode. The Cs of the electrode material decreased from 302 to 270.6 F/g with the increase in current density. The retention rate of the Cs of MnO_2/NG was 89.6%, indicating good performance of the material for supercapacitors. The Cs of charge and discharge decreased with the increase in current density, mainly because the oxidation rate of active substances and diffusion of charge cannot satisfy the rapid growth of current density.

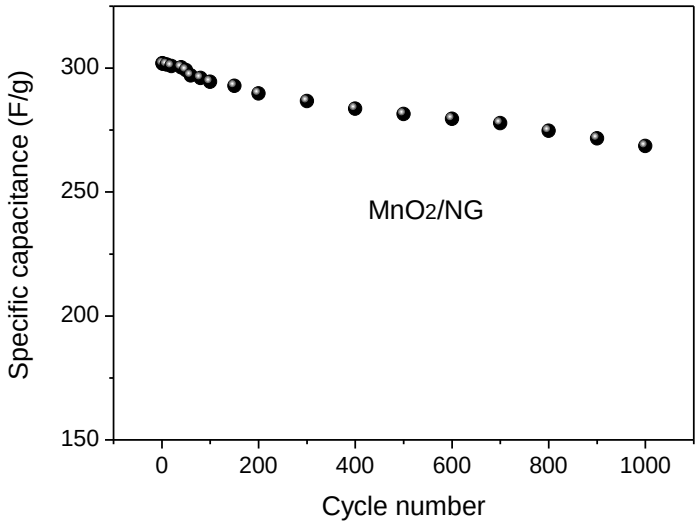

Figure 5. Cycling stability of the MnO_2/NG electrode measured at 1 A/g.

The MnO_2/NG composite also shows excellent cycling stability, assessed by a GCD test at 1 A/g for 1000 cycles as shown in Figure 5. In the first cycle, the coulombic efficiency slightly decreased to 302 F/g with almost 100% conversion. After 1000 cycles, the Cs was still as high as ~268.6 F/g, slightly less than that of the first cycle. This is mainly because of the loss of active

materials in electrodes and/or the mass loss of the electrode. The above analyses clearly show that the capacitance retention can be largely maintained (88.9%) for MnO_2/NG composite after 1000 cycles, indicating superior electrochemical stability of such electrode materials. For this point, we assume that the improved electrochemical stability for MnO_2/NG composite is mainly because the well-dispersed nanosized MnO_2 NPs on the surface of NG significantly decreased the diffusion of Na^+ ions during the charge/discharge process. In addition, the excellent conductivity of NG is also beneficial for providing the electronic conductive bridges for electrochemical path.

The current material was compared with other materials reported in the literature as shown in Table 1. The MnO_2/NG composites reported in this paper showed good electrochemical activity and could be used for supercapacitor applications. The excellent capacitance achieved in our study can be attributed to the following two advantages: First, excellent intrinsic electrical properties of graphene that acts as both an electron conductor and a volume buffer layer, and second, nitrogen doping that provides a higher number of active sites by increasing the Fermi level towards the conduction band, thus leading to excellent electrochemical performance. On the other hand, highly dispersed MnO_2 particles with a mean size of about 10–20 nm on NG nanosheets provide sufficient electrochemically active sites for effective redox reactions on the surface of MnO_2.

Table 1. Comparison of Cs with other MnO_2-based electrodes

Electrode Materials	Cs (F/g)	Scan rate or current density	Electrolyte	References
B-RGO/MnO_2	248.5	10 mV/s	1M Na_2SO_4	[24]
MnO_2/C	165	5 mV/s	0.5M Na_2SO_4	[25]
graphene–MnO_2	310	2 mV/s	1M Na_2SO_4	[26]
MnO_2/MWNT	285.12	1.0 A/g	1M Na_2SO_4	[27]
MnO_2/C/G	255	0.5 A/g	1M Na_2SO_4	[28]
MnO_2/C/G	150	20 A/g	1M Na_2SO_4	[28]
GW-MnO_2	210	0.5 A/g	1M Na_2SO_4	[29]
MnO_2@AMC	297.8	0.2 A/g	1M Na_2SO_4	[30]
MnO_2/NG	302	1.0 A/g	1M Na_2SO_4	This work

ABBREVIATIONS:

B-RGO/MnO_2: birnessite-type MnO_2/graphene nanocomposites, MnO_2/C/G: honeycomb MnO_2 nanospheres/carbon nanoparticles/graphene composites, GW-MnO_2: graphene-wrapped MnO_2 nanocomposites, MnO_2@AMC: flower-like MnO_2 coated activated multihole carbon (MnO_2@AMC)

4. CONCLUSION

In summary, MnO_2/NG nanocomposites were efficiently synthesized via a PVP-assisted ethylene glycol solvothermal process. The as-prepared products exhibited a superior electrochemical performance for supercapacitors. Owing to the synergistic effect between the pseudocapacitance of

MnO_2 NPs and good electrical conductivity of NG nanosheets, the MnO_2/NG electrode materials showed enhanced capacitive performance of as high as 302 F/g at 1.0 A/g. The capacitance retention was largely maintained (88.9%) for the MnO_2/NG composite after 1000 cycles, indicating satisfactory potential application of the composites as high-performance supercapacitors. This study provides a promising electrode material for supercapacitors with excellent activity and enhanced durability.

ACKNOWLEDGEMENT
This work is funded by the Open Project Program of Jiangxi Engineering Research Center of Process and Equipment for New Energy, East China University of Technology (JXNE2016-02) and Nature Science Foundation of Jiangxi Province (2015ZBAB203002).

References

1. L. Dong, Z. Chen, D. Yang and H. Lu, *RSC Adv.*, 3 (2013) 21183.
2. J. Miller and P. Simon, *Science*, 321 (2008) 651.
3. L.L. Zhang and X.S. Zhao, *Chem. Soc. Rev.*, 38 (2009) 2520.
4. T.Y. Wei, C.H. Chen, H.C. Chien, S.Y. Lu and C.C. Hu, *Adv. Mater.*, 22 (2010) 347.
5. P. Simon, Y. Gogotsi, *Nat. Mater.*, 7 (2008) 845.
6. Y. Chen, X. Zhang, D. Zhang, P. Yu and Y. Ma, *Carbon*, 49 (2011) 573.
7. D. Zhang, X. Zhang, Y. Chen, P. Yu, C. Wang and Y. Ma, *J. Power Sources*, 196 (2011) 5990.
8. S. Chen, J. Zhu, X. Wu and Q. Han, *ACS Nano*, 4 (2010) 2822.
9. L. Yang, S. Cheng, X. Ji, Y. Jiang, J. Zhou and M. Liu, *J. Mater. Chem. A*, 3 (2015) 7338.
10. C.H. Yang, I.W. Sun, C.T. Hsieh, T.Y. Wu, C.Y. Su, Y.S. Li and J.K. Chang, *J. Mater. Chem. A*, 4 (2016) 4015.
11. L. Bao, T. Li, S. Chen, C. Peng, L. Li, Q. Xu, Y.H. Chen, E.C. Ou and W.J. Xu, *Small*, 13 (2017) 1602077.
12. B. Bayatsarmadi, Y. Zheng, A. Vasileff and S.Z. Qiao, *Small*, 13 (2017) 1700191.
13. W. Wei, X. Cui, W. Chen and D. G. Ivey, *Chem. Soc. Rev.*, 40 (2011) 1697.
14. Y. Qian, C.L. Huang, R. Chen, S.Z. Dai and C.Y. Wang, *Int. J. Electrochem. Sci.*, 11 (2016) 7453.
15. H. Chen, J. He, C. Zhang and H. He, *J. Phys. Chem. C*, 111 (2007) 18033.
16. C. Yu, L. Zhang, J. Shi, J. Zhao, J. Gao and D. Yan, *Adv. Funct. Mater.*, 18 (2008), 1544.
17. J.B. Fei, Y. Cui, X.H. Yan, W. Qi, Y. Yang, K.W. Wang, Q. He and J.B. Li, *Adv. Mater.*, 20 (2008) 452.
18. A.E. Fischer, K.A. Pettigrew, D.R. Rolison, R.M. Stroud and J.W. Long, *Nano Lett.*, 7 (2007) 281.
19. J.H. Kim, K.H. Lee, L.J. Overzet and G.S. Lee, *Nano Lett.*, 11 (2011) 2611.
20. K.S. Novoselov, A.K. Geim, S.V. Morozov, D. Jiang, Y. Zhang, S .V. Dubonos, I.V. Grigorieva, and A.A. Firsov, *Science*, 306 (2004) 666.
21. B.G. Sumpter, V. Meunier, J.M. Romo-Herrera, E. Cruz-Silva, D.A. Cullen, H. Terrones, D. J Smith and M. Terrones, *ACS Nano*, 1 (2007) 369.
22. D.W. Chang, E. K. Lee, E.Y. Park, H.J. Yu, H.J. Choi, In.Y. Jeon, G.J. Sohn, D.B. Shin, N.J. Park, J.H. Oh, L.M. Dai and J.B. Baek, *J. Am. Chem. Soc.*, 135 (2013) 8981.
23. Z.P. Li, J.Q. Wang, S. Liu, X. H Liu and S.R. Yang, *Journal of Power Sources*, 196 (2011) 8160.
24. M. Kim, Y. Hwang, J. Kim, *J. Mater. Sci.* 48(2013) 7652.
25. R.K. Sharma, H.S. Oh, Y.G. Shul, H. Kim, *Journal of Power Sources* 173 (2007) 1024.
26. J. Yan, Z. Fan, T. Wei, W. Qian, M. Zhang, F. Wei, *Carbon* 48 (2010) 3825.
27. Y. Qian, C. Huang, R. Chen, S. Dai, C. Wang, *Int. J. Electrochem. Sci.*, 11 (2016) 7453.

28. Y. Xiong, M. Zhou, H. Chen, L. Feng, Z. Wang, X. Yan, S. Guan, *Applied Surface Science* 357 (2015) 1024.
29. J. Zhu, J. He, *ACS Appl. Mater. Interfaces* 2012, 4, 1770−1776
30. S. Zhu, W. Cen, L. Hao, J. Ma, L. Yu, H. Zheng, Y. Zhang, *Materials Letters* 135 (2014) 11.